Article

Discovery Medicine 2024; 36(187): 1743–1757
https://doi.org/10.24976/Discov.Med.202436187.160

Regulation of Nrf2/A20/eEF1A2 Axis by Ginsenoside Rb1: A Key Pathway in Alleviating Cerebral Ischemia-Reperfusion Injury

Haijuan He[1,2,†], Yanqing Yang[1,†], Xia Zhang[1], Ying Ying[1], Bo Zheng[1,2,*]

[1]Department of Anesthesiology, Taizhou Hospital of Zhejiang Province Affiliated to Wenzhou Medical University, 317000 Taizhou, Zhejiang, China
[2]Department of Anesthesiology, Luqiao Hospital, Taizhou Enze Medical Center (Group), 318050 Taizhou, Zhejiang, China
*Correspondence: zhengbo@enzemed.com (Bo Zheng)
[†]These authors contributed equally.
Published: 20 August 2024

Background: Cerebral ischemia-reperfusion injury (CIRI) is a prevalent neurological disorder, characterized by the oxidative stress and inflammatory response induced during the ischemia-reperfusion process, leading to significant damage to brain cells. Ginsenoside Rb1, a natural medicinal ingredient, possesses potential neuroprotective effects. This study aims to investigate the mechanism of action of ginsenoside Rb1 in CIRI and its protective effects on brain injury.

Methods: We utilized a mouse CIRI model and randomly divided the mice into control group, CIRI group, and ginsenoside Rb1 treatment group. The effects of Rb1 on brain tissue damage, apoptosis, expression of inflammatory factors, and pyroptotic cell numbers in CIRI mice were observed through triphenyl tetrazolium chloride (TTC) staining, terminal deoxynucleotidyl transferase dUTP nick end labeling (TUNEL) staining, real-time reverse transcription polymerase chain reaction (qRT-PCR), and electron microscopy. In a cell model, the regulatory effect of Rb1 on oxygen-glucose deprivation/reperfusion (OGD/R)-induced HT22 cell pyroptosis via the nuclear respiratoty factor 2/tumor necrosis factor-α (TNF-α)-induced Protein 3 (TNFAIP3, aka A20)/eukaryotic translation elongation factor 1A2 (Nrf2/A20/eEF1A2) axis was detected using Western blot and TUNEL staining. Additionally, the impact of Nrf2 inhibitor ML385 and eEF1A2 overexpression on the neuroprotective effect of Rb1 was assessed. Using the comprehensive experimental methods mentioned above, the neuroprotective mechanism of Rb1 in CIRI was thoroughly evaluated.

Results: Our findings demonstrate that treatment with ginsenoside Rb1 alleviated behavioral deficits induced by CIRI and reduced pathological damage in brain tissue. Furthermore, ginsenoside Rb1 treatment notably decreased oxidative stress and the inflammatory response induced by CIRI, leading to lower levels of inflammatory factors ($p < 0.05$). Further experimental results indicated that ginsenoside Rb1 promoted antioxidant and anti-inflammatory responses by regulating the activity of the Nrf2/A20/eEF1A2 axis. Additionally, ginsenoside Rb1 inhibited the activation of the NOD-like receptor thermal protein domain associated protein 3 (NLRP3) inflammasome, thereby reducing the release of inflammatory factors and the occurrence of cell apoptosis.

Conclusion: Our study results suggest that ginsenoside Rb1 exerts neuroprotective effects and alleviates brain injury induced by CIRI by regulating the Nrf2/A20/eEF1A2 axis and inhibiting the activation of the NLRP3 inflammasome. These findings provide new treatment insights for CIRI and support ginsenoside Rb1's development as a therapeutic drug. However, despite the promising nature of our findings, further research is required to validate these discoveries and explore the feasibility and safety of ginsenoside Rb1 in clinical applications. We hope that our study can provide new directions and strategies for the treatment and prevention of CIRI, contributing to the development of neuroprotective drugs.

Keywords: CIRI; ginsenoside Rb1; Nrf2/A20/eEF1A2 axis; NLRP3; neuroprotection

Introduction

Cerebral ischemia-reperfusion injury (CIRI) is a common and severe neurological disorder characterized by the restoration of blood flow following cerebral vascular occlusion, triggering a series of pathophysiological responses that lead to neuronal damage and death [1–3]. In recent years, studies have revealed the significant roles of the Nrf2/A20/eEF1A2 axis and the NOD-like receptor thermal protein domain associated protein 3 (NLRP3) inflammasome in CIRI [4–7]. However, precise regulation of these molecular pathways to alleviate CIRI remains an unresolved issue. Additionally, pyroptosis, as a novel form of cell death, and its role and mechanisms in CIRI are current hotspots and challenges in research [8,9].

Ginsenoside Rb1 has been found in recent studies to possess multiple biological activities, including antiox-

idative, anti-inflammatory, and anti-apoptotic effects [10–12]. Specifically, some research has indicated that ginsenoside Rb1 can regulate Nrf2 and NLRP3, thereby inhibiting pyroptosis and alleviating CIRI [13,14]. Furthermore, ginsenoside Rb1 has been found to modulate multiple signaling pathways such as phosphatidylinositol-3-kinase (PI3K)/Akt and mitogen-activated protein kinase (MAPK), demonstrating its broad biological activity and potential pharmacological effects [15,16]. However, the precise regulatory mechanisms of ginsenoside Rb1 on the Nrf2/A20/eEF1A2 axis and NLRP3 pathways have not been fully elucidated. Although the neuroprotective effects of ginsenoside Rb1 and its potential mechanisms have been studied to a certain extent, its specific role in CIRI and the detailed mechanisms of its regulation of the Nrf2/A20/eEF1A2 axis and NLRP3, particularly its role in inhibiting pyroptosis, remain unclear. Furthermore, whether ginsenoside Rb1 may exert neuroprotective effects through other unknown mechanisms is also a topic worthy of further exploration.

In this study, utilizing *in vitro* cell models and *in vivo* animal models, we systematically investigated the role of ginsenoside Rb1 in CIRI and its potential mechanisms. We found that ginsenoside Rb1 effectively regulates the Nrf2/A20/eEF1A2 axis and NLRP3, inhibits pyroptosis, and alleviates CIRI. These findings provide an important theoretical basis for a deeper understanding of the pathogenesis of CIRI and the development of new treatment strategies. Additionally, we will explore other potential neuroprotective mechanisms of ginsenoside Rb1, aiming to provide further scientific basis for the clinical application of traditional Chinese medicine.

Materials and Methods

Animal Model

Forty-five male SPF-grade C57BL/6 mice (6-week-old, weighing 18–22 g), obtained from Beijing Vital River Laboratory Animal Technology Co., Ltd. (Beijing, China) with license number SCXK (Jing) 2016-0006, were housed in a barrier facility with *ad libitum* access to food and water. The temperature and humidity were maintained at 23 ± 1 °C and 50 ± 10%, respectively, with a 12-hour light/dark cycle. Experimental methods followed protocols outlined by Yang *et al.* [17] and Li *et al.* [18], with slight modifications. The focal cerebral ischemia-reperfusion model was induced using the middle cerebral artery occlusion (MCAO) method. Mice were anesthetized with 1% pentobarbital sodium at a dose of 40 mg/kg. A midline incision in the neck exposed the left common carotid artery. Of the 45 mice, 30 successfully underwent surgery for use in subsequent experiments.

The internal and external branches of the carotid artery were identified and separated, with the distal portion of the external carotid artery subsequently being ligated. Both the common carotid artery and the internal carotid artery were then temporarily clamped. A nylon suture was inserted through the incision until resistance was felt, indicating successful occlusion, and then tied below the level of the initial incision. Subsequently, the clamps on the artery were released. The time of ischemia onset was recorded, and after 2 hours, the suture was removed, and the wound was sutured closed. Laser Speckle Contrast Imaging (LSCI) was employed to monitor changes in cerebral blood flow (CBF), confirming the successful establishment of the ischemia-reperfusion (I/R) model.

During the operation, the temperature was maintained at 37 ± 0.5 °C. After the procedure, mice were euthanized via cervical dislocation following inhalation of 4% isoflurane. The mortality rate among mice undergoing the procedure was 24.7%. Mice that successfully underwent the procedure were randomly assigned to the Sham group, Model group, and 50 mg/kg ginsenoside Rb1 group [19–21], with 10 mice in each group. The Sham operation mirrored the Model group procedure, except for the absence of nylon thread insertion to block blood flow. Throughout the reperfusion period, both the Sham and MCAO groups received intraperitoneal injections of saline, while the Rb1 group received intraperitoneal injections of Rb1.

Triphenyl Tetrazolium Chloride (TTC) Staining

After drug administration, whole brains were immediately removed from mice anesthetized with 4% pentobarbital sodium intraperitoneally. The brains were rinsed with pre-cooled 1×PBS, blotted dry with filter paper, and divided into two portions. One portion of the brain tissue was frozen at –20 °C for 30 min, then sliced into 5 sections (2 mm thick) on ice. The sections were placed in 2% TTC staining solution, covered with aluminum foil, and incubated at 37 °C for 30 min. The brain tissue sections were flipped to ensure even contact with the staining solution. After washing the sections with PBS for 3–5 min, images were immediately captured.

TUNEL Staining for Detection of Neuronal Apoptosis

Brain specimens, preserved in 4% paraformaldehyde, were encased in paraffin before being sliced into sections 5 micrometers in thickness. The sections underwent sequential processing, including baking, deparaffinization in xylene, hydration in graded ethanol, and washing, followed by incubation with proteinase K (40308-D, YEASEN, Shanghai, China) at 37 °C for 25 min and subsequent washing with PBS. Terminal deoxynucleotidyl transferase dUTP nick end labeling (TUNEL) detection solution was added and incubated at 37 °C for 60 min. DAPI staining was then added, followed by a 10-minute light-protected reaction. After PBS washing and air-drying, the sections were mounted with anti-fluorescence quenching mounting medium. Three random fields were captured for each section, and the apoptosis index (AI) was calculated using Im-

Table 1. PCR sequence in this study.

	Forward	Reverse
IL-1β	5′-TTGACGGACCCCAAAAGATG-3′	5′-AGAAGGTGCTCATGTCCTCA-3′
IL-6	5′-GTTCTCTGGGAAATCGTGGA-3′	5′-TGTACTCCAGGTAGCTATGG-3′
TNF-α	5′-TCTCATCAGTTCTATGGCCC-3′	5′-GGGAGTAGACAAGGTACAAC-3′
GAPDH	5′-GTCGTGGAGTCTACTGGCGTCTTCA-3′	5′-TCGTGGTTCACACCCATCACAAACA-3′

IL, interleukin; *TNF-α*, tumor necrosis factor-α; *GAPDH*, glyceraldehyde-3-phosphate dehydrogenase.

ageJ image analysis software (ImageJ 1.8.0, U. S. National Institutes of Health, Bethesda, MD, USA), where AI (%) = (number of apoptotic cells ÷ total number of cells) × 100%. TTC staining revealed red for normal tissue and white for the infarct area.

qRT-PCR Analysis

100 mg of tissue from the cerebral cortex underwent a series of procedures, starting with the extraction of total RNA, followed by a reverse transcription process, and culminating in a real-time reverse transcription polymerase chain reaction (qRT-PCR) using fluorescence detection. The reaction mixture comprised 2 × 2.5 µL of a specialized mix for real-time reverse transcription polymerase chain reaction, 2 µL of specific gene primers, 1 µL of the synthesized cDNA, and 2 µL of double-distilled water. The amplification protocol included an initial denaturation at 95 °C for one minute, followed by 40 cycles of denaturation at 95 °C for 20 s and annealing/extension at 60 °C for 1 min. To analyze the qRT-PCR products, a melting curve analysis was conducted by gradually increasing the temperature from 60 °C to 95 °C at increments of 0.3 °C every 15 s. The housekeeping gene glyceraldehyde-3-phosphate dehydrogenase (*GAPDH*) served as the control for normalization (Table 1), and the $2^{-\Delta\Delta CT}$ method was employed to determine the relative expression levels of the gene of interest.

HT22 Cell Culture

HT22 cells (BFN60808571) were obtained from the American Type Culture Collection (ATCC, Manassas, VA, USA). They were confirmed to be mycoplasma-free, and STR analysis revealed their derivation from parental cells. HT22 cells were cultured in DMEM supplemented with 10% FBS. The culture medium was refreshed every 2 days, and cell passaging was performed when the confluency reached approximately 90% following digestion with 0.25% trypsin. Cells from the 7th generation were selected for subsequent studies in this research.

Preparation, Grouping, and Drug Administration in the OGD/R Model

The experiment consisted of a control group, an oxygen-glucose deprivation/reperfusion (OGD/R) group, and an Rb1 administration group. In the control group, cells were routinely cultured in complete culture medium for 24 hours. In the OGD/R group, cells were cultured in DMEM sugar-free medium at 37 °C in a constant temperature anaerobic culture box (95% N_2, 5% CO_2) for 3 h, followed by routine culture in complete culture medium to establish the OGD/R cell injury model. In the Rb1 group, cells were first subjected to anaerobic culture for 3 h, similar to the OGD/R group, and then cultured in complete culture medium containing 10 µmol/L Rb1 for 24 h. The Rb1 dosage was determined based on literature references and preliminary experiments conducted by the research group. Plasmids were obtained from Guangzhou Ribobio Company (15313134204, Guangzhou, China). When HT22 cell growth reached 70% to 80% confluence, plasmids were transfected into the cells using Lipofectamine 3000 (L3000015, Thermo Fisher Scientific Inc., Waltham, MA, USA) according to the instructions (eEF1A2 forwards 5′-TCGAATCTCCCTCTGGAAGTT-3′, reversed 5′-CTTGAACCACGGCATGTTG-3′). Subsequent experiments were conducted 24 to 48 h after cultivation.

Nuclear Protein Extraction

Nuclear and cytoplasmic proteins were extracted using the NE-PER™ Nuclear and Cytoplasmic Extraction Reagent Kit (Catalog number: 78833, Thermo Fisher Scientific Inc., Waltham, MA, USA). The NE-PER kit employs a method for nuclear protein extraction involving a simple, step-by-step process of cell lysis followed by centrifugal separation of nuclear and cytoplasmic protein components. The NE-PER reagents efficiently solubilize and separate various cytoplasmic and nuclear proteins into aliquots, resulting in minimal cross-contamination or interference from genomic DNA and mRNA. Once desalted or diluted, the separated proteins can be utilized for immunodetection experiments.

Western Blot

Total protein was isolated from mouse brain tissue and HT22 cells using RIPA buffer (20201ES60, YEASEN, Shanghai, China). The protein content was quantified using the BCA assay (20201ES76, YEASEN, Shanghai, China). Proteins were then separated by 10% SDS-PAGE and transferred to a membrane via electrophoretic transfer (1658004, Bio-Rad, Hercules, CA, USA). The membrane was blocked with 5% skim milk in TBST for 1 h. Primary antibodies targeting NOD-like receptor thermal protein domain

associated protein 3 (NLRP3) (#15101, 1:1000, Cell Signaling Technology, Inc., Beverly, MA, USA), apoptosis-associated speck-like protein containing a CARD (ASC) (#67824, 1:1000, CST, Beverly, MA, USA), Gasdermin-D (GSDMD)-N (#39754, 1:1000, CST, Beverly, MA, USA), Cleaved-Caspase-1 (#89332, 1:1000, CST, Beverly, MA, USA), interleukin-1β (IL-1β) (#BF8021, 1:1000, Affinity, Jiangsu, China), IL-18 (#DF6252, 1:1000, Affinity, Jiangsu, China), and β-actin (#4967, 1:1000, CST, Beverly, MA, USA) were applied and incubated overnight at 4 °C. Secondary antibodies, goat anti-mouse IgG (#7076, 1:3000, CST, Beverly, MA, USA) and goat anti-rabbit IgG (#7074, 1:3000, CST, Beverly, MA, USA), were applied and incubated at room temperature for 1 h the following day. The proteins were visualized using enhanced chemiluminescence (ECL) detection (36208ES60, Super ECL Detection Reagent, YESEN, Shanghai, China), and the intensity of the bands was quantified with ImageJ software (v1.8.0.345, National Institutes of Health, Bethesda, MD, USA).

Transmission Electron Microscopy

Brain cortex tissue, fixed in electron microscopy fixative, underwent acid fixation, followed by washing with PBS three times and dehydration in graded ethanol. Subsequently, infiltration with acetone, embedding, and preparation of ultrathin sections (70 nm thick) was performed. Uranium-lead double staining was carried out for 15 min each. The sections were air-dried at room temperature overnight. Finally, the slices were examined under a transmission electron microscope (F200X S, Thermo Fisher Scientific, Waltham, MA, USA) to assess the situation of neuronal cell necrosis based on the ultrastructure.

Statistical Analysis

The analysis of the data was conducted using SPSS software, version 26.0 (IBM Corp., Armonk, NY, USA), while statistical charts were created using GraphPad Prism, version 8.0 (GraphPad Software, Inc., San Diego, CA, USA). Western blot results were analyzed using Image J software (v1.8.0.345, National Institutes of Health, Bethesda, MD, USA). Data from measurements were presented as the mean $\pm$ standard deviation. To assess differences among several groups, one-way ANOVA was employed, followed by the LSD test for post-hoc multiple comparisons. A p value below 0.05 was considered to indicate a statistically significant difference.

Results

Animal Experiments Confirmed the Role of Rb1 in Reducing CIRI

TTC staining serves as a common method for staining neural tissue to evaluate the extent of neuronal cell necrosis following ischemia-reperfusion injury. In our experiment, no obvious necrotic areas were observed in the Sham group. Notably, the area of necrotic tissue in the I/R+Rb1 group was smaller than that in the I/R group, suggesting that Rb1 can mitigate the extent of neuronal cell necrosis (Fig. 1A). TUNEL staining is frequently employed to detect cell apoptosis. Our experimental results revealed a significant reduction in the number of TUNEL-positive cells in the I/R+Rb1 group compared to the I/R group, indicating that Rb1 can attenuate the extent of neuronal cell apoptosis (Fig. 1B, $p < 0.01$). Furthermore, we utilized qRT-PCR to examine the expression levels of inflammatory factors tumor necrosis factor-α (*TNF-*α), *IL-1*β, and *IL-6*. The findings demonstrated significantly lower expression levels of *TNF-*α, *IL-1*β, and *IL-6* in the I/R+Rb1 group compared to the I/R group (Fig. 1C–E, $p < 0.05$). This suggests that Rb1 can suppress the expression of inflammatory factors.

Ginsenoside Rb1 Alleviates Mouse CIRI by Inhibiting Pyroptosis

Caspase-1 serves as a crucial inflammatory caspase that undergoes cleavage into its active form following inflammasome activation, thereby mediating the maturation and release of IL-1β and IL-18. In the I/R group, the expression levels of NLRP3, ASC, GSDMD-N, Cleaved-Caspase-1, IL-1β, and IL-18 were upregulated significantly ($p < 0.01$). Following Rb1 treatment, this significant increase trend was reversed ($p < 0.01$) (Fig. 2A–G, $p < 0.05$), indicating that Rb1 can inhibit the expression of these inflammation- and pyroptosis-related molecules. Electron microscopy (F200X S, Thermo Fisher Scientific, Waltham, MA, USA) experiments corroborated these findings, demonstrating that the number of pyroptotic cells in the I/R+Rb1 group was lower than that in the I/R group, further underscoring the inhibitory effect of Rb1 on pyroptosis (Fig. 2H). In conclusion, based on the comprehensive experimental results, it can be inferred that ginsenoside Rb1 mitigates CIRI by reducing the expression of pyroptosis-related proteins.

Cell Model Results also Show that Ginsenoside Rb1 can Inhibit Pyroptosis in HT22 Cells

Subsequently, we employed an OGD/R model to simulate CIRI and investigated the regulatory effect of ginsenoside Rb1 on NLRP3 inflammasomes. In the cell model, our experimental results demonstrate that ginsenoside Rb1 can effectively inhibit pyroptosis in HT22 cells. Fig. 3A illustrates pyroptosis proteins, which play pivotal roles in inflammatory responses and cell apoptosis. The findings indicate a significant decrease in pyroptosis proteins in the Rb1-treated group (OGD/R+Rb1 group) compared to the OGD/R group ($p < 0.01$). This suggests that ginsenoside Rb1 may impede the activation of NLRP3 inflammasomes, thereby reducing cell pyroptosis and inflammatory responses (Fig. 3B–G). Furthermore, TUNEL staining results reveal a noteworthy reduction in TUNEL-positive

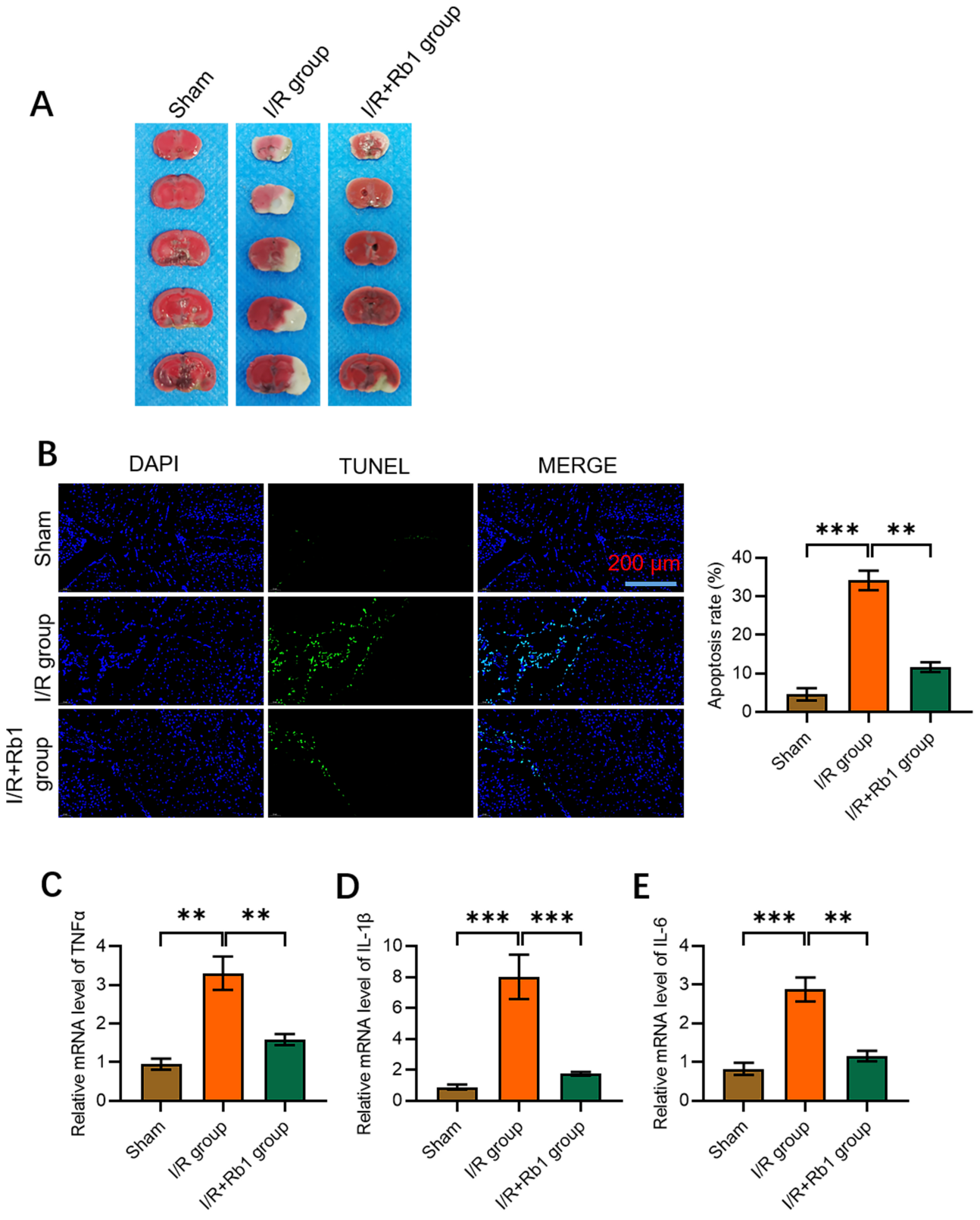

Fig. 1. Verification of the neuroprotective role of Rb1 in cerebral ischemia-reperfusion injury (CIRI) animal model. (A) Triphenyl tetrazolium chloride (TTC) staining confirmed the neuroprotective effect of Rb1. (B) Terminal deoxynucleotidyl transferase dUTP nick end labeling (TUNEL) staining confirmed the reduction of neuronal apoptosis by Rb1, 200×. (C–E) Real-time reverse transcription polymerase chain reaction (qRT-PCR) analysis revealed the inhibition of inflammatory factors *TNF-α* (C), *IL-1β* (D), and *IL-6* (E) expression by Rb1. N = 10, $^{**}p < 0.01$, $^{***}p < 0.001$. I/R, ischemia-reperfusion.

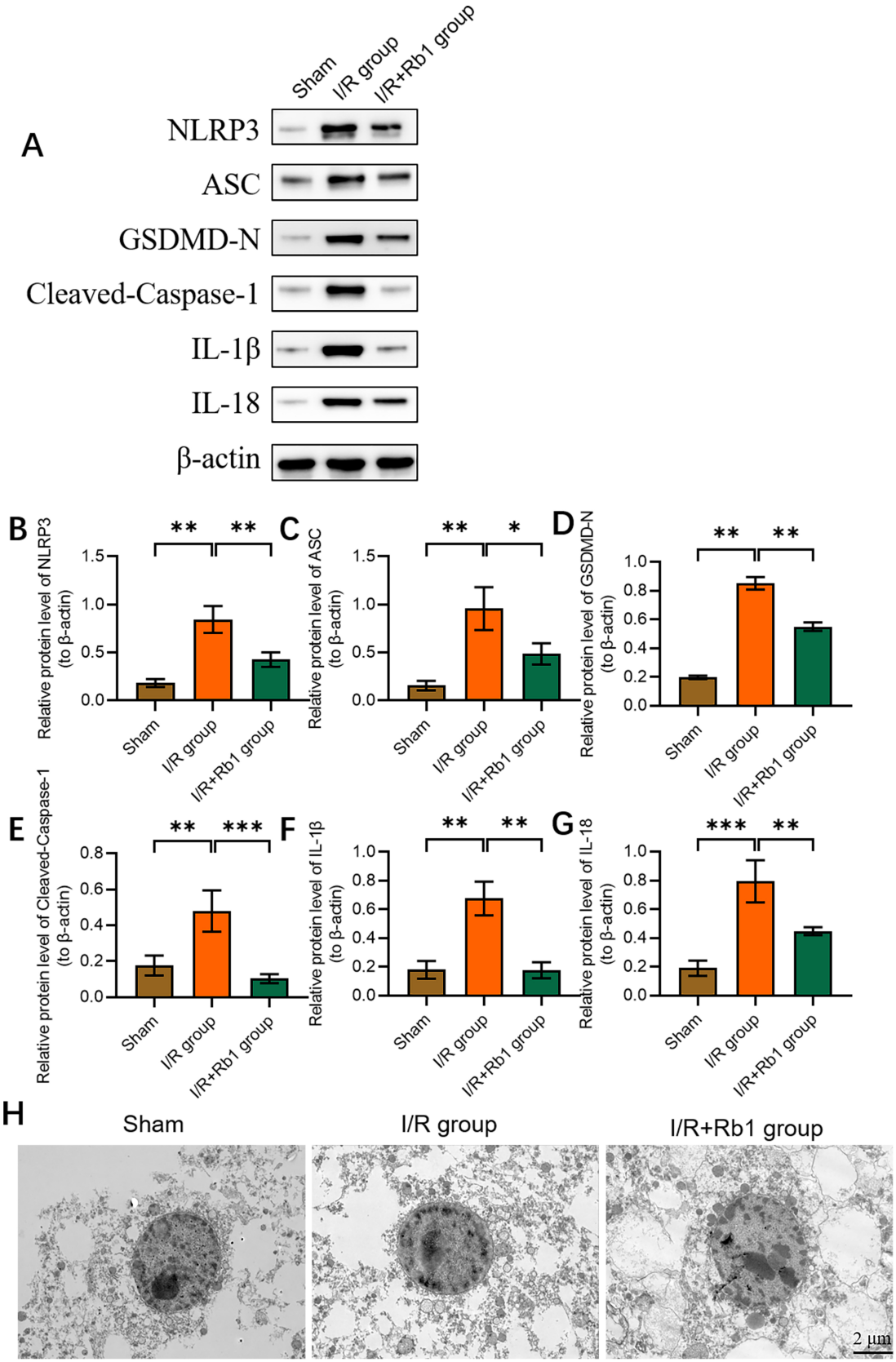

Fig. 2. Ginsenoside Rb1 alleviates CIRI in mice by inhibiting pyroptosis. (A–G) Western blot images of NOD-like receptor thermal protein domain associated protein 3 (NLRP3), apoptosis-associated speck-like protein containing a CARD (ASC), Gasdermin-D (GSDMD)-N, Cleaved-Caspase-1, IL-1β, IL-18, and β-actin protein expression. (H) Electron microscopy confirmed the inhibition of pyroptosis by Rb1, 4000×. N = 10, *$p < 0.05$, **$p < 0.01$, ***$p < 0.001$.

cells in the ginsenoside Rb1-treated group, further affirming the protective effect of ginsenoside Rb1 in reducing apoptosis in HT22 neuronal cells (Fig. 3H, $p < 0.01$).

Ginsenoside Rb1 Increases the Expression of Nrf2 in OGD/R-damaged Neurons

This section elucidates the impact of ginsenoside Rb1 on the expression of nuclear respiratoty factor 2 (Nrf2) in OGD/R-damaged neurons using Western blot analysis, encompassing Nrf2 in both the cytoplasm and nucleus. Fig. 4A illustrates the upregulation of Nrf2 expression in both the cytoplasm and nucleus following treatment with Rb1. According to the experimental findings, the total expression of Nrf2 exhibits a notable increase in the Rb1-treated group (OGD/R+Rb1 group) compared to the OGD/R group (Fig. 4B, $p < 0.01$). Moreover, in both the cytoplasm and nucleus, the Rb1-treated group demonstrates significantly elevated levels of Cyto-Nrf2 and Nuc-Nrf2 compared to the OGD/R group, indicating that ginsenoside Rb1 effectively enhances the expression of Nrf2 in both cellular compartments (Fig. 4C,D, $p < 0.05$).

Ginsenoside Rb1 Increases the Expression of A20 and Inhibits the Expression of eEF1A2 and p-p65

Fig. 5A illustrates the alterations in various proteins. Tumor necrosis factor-α (TNF-α)-induced Protein 3 (TNFAIP3, aka A20), recognized as an anti-inflammatory factor, typically exhibits upregulation associated with anti-inflammatory and cytoprotective effects. The OGD/R group (oxygen-glucose deprivation/reperfusion model group) displays a significant increase in A20 expression ($p < 0.01$), likely indicative of a cellular stress response to ischemia-reperfusion injury. Notably, the OGD/R+Rb1 group demonstrates a further increase in A20 expression ($p < 0.05$), suggesting that ginsenoside Rb1 may confer a protective effect by augmenting A20 expression (Fig. 5B). Eukaryotic translation elongation factor 1A2 (eEF1A2), an enzyme implicated in protein synthesis, may experience overexpression in association with cellular stress and damage. In contrast, the OGD/R group exhibits a significant decrease in eEF1A2 expression ($p < 0.05$), possibly attributable to the impact of ischemia-reperfusion injury on protein synthesis. Remarkably, the OGD/R+Rb1 group manifests a significant decrease in eEF1A2 expression (Fig. 5C, $p < 0.01$). P65, a subunit of the nuclear factor kappa-B (NF-κB) transcription factor, is typically associated with inflammatory responses and cell survival. Phosphor (p)-p65 represents the phosphorylated form of p65, signifying the activated state of NF-κB and its involvement in pro-inflammatory responses. In the OGD/R group, there is a significant increase in p-p65 expression ($p < 0.01$), while the total expression of p65 remains unaltered, indicative of NF-κB activation by ischemia-reperfusion. Conversely, the OGD/R+Rb1 group demonstrates a noteworthy reduction in p-p65 expression to baseline levels ($p < 0.05$), while the total expression of p65 remains unchanged (Fig. 5D). In summary, the experimental findings suggest that ginsenoside Rb1 may mitigate CIRI induced by OGD/R through upregulating A20 expression and inhibiting eEF1A2 activation. Moreover, Rb1 may attenuate the inflammatory response by inhibiting NF-κB activation.

The Nrf2 Inhibitor ML385 Reverses the Protective Effect of Ginsenoside Rb1 on HT22 Cells after OGD/R Injury

Nrf2 serves as a pivotal transcription factor pivotal in cellular responses to oxidative stress and inflammatory reactions. In this experiment, Nrf2 exhibited distinct changes across different treatment groups, reflecting the diverse responses of cells to oxygen-glucose deprivation/reperfusion, as well as the administration of ginsenoside Rb1 and the Nrf2 inhibitor ML385. The OGD/R group (oxygen-glucose deprivation/reperfusion model group) demonstrated increased Nrf2 expression, suggesting that cells may elevate Nrf2 levels to counteract oxidative stress induced by oxygen-glucose deprivation. Conversely, the OGD/R+Rb1 group (ginsenoside Rb1 treatment group) displayed further augmented Nrf2 expression, indicative of Rb1 potentially conferring protective effects by enhancing Nrf2 expression. Intriguingly, the OGD/R+Rb1+ML385 group (ML385 combined with Rb1 treatment) exhibited a notable reduction in Nrf2 expression to baseline levels ($p < 0.001$), signifying the effective inhibition of Rb1-induced Nrf2 upregulation by ML385 (Fig. 6A,B).

In the oxygen-glucose deprivation/reperfusion model, there was a significant increase in the expression of NLRP3, ASC, GSDMD-N, and Cleaved-Caspase-1 ($p < 0.01$), indicating the activation of the inflammasome and pyroptotic pathways. Ginsenoside Rb1 treatment notably reduced the expression of NLRP3, ASC, and GSDMD-N, while restoring the expression of Cleaved-Caspase-1 to baseline levels ($p < 0.05$), suggesting that Rb1 may confer protective effects by inhibiting the activation of the NLRP3 inflammasome and pyroptotic pathways. However, when the Nrf2 inhibitor ML385 was combined with Rb1 treatment, there was a significant increase in NLRP3 and ASC expression ($p < 0.05$), with GSDMD-N expression remaining elevated, and Cleaved-Caspase-1 expression also rising significantly ($p < 0.001$). This indicates that ML385 reversed the protective effect of Rb1, leading to the reactivation of the inflammasome and pyroptotic pathways (Fig. 6C–F).

Overexpression of eEF1A2 Reduces the Protective Effect of Ginsenoside Rb1 on HT22 Cells after OGD/R Injury

In this experiment, the successful overexpression of eEF1A2 was confirmed by observing a significant increase in eEF1A2 expression in the OE-eEF1A2 group ($p < 0.01$), indicating successful transfection of the eEF1A2 overexpression plasmid (Fig. 7A,B). Subsequently, changes in

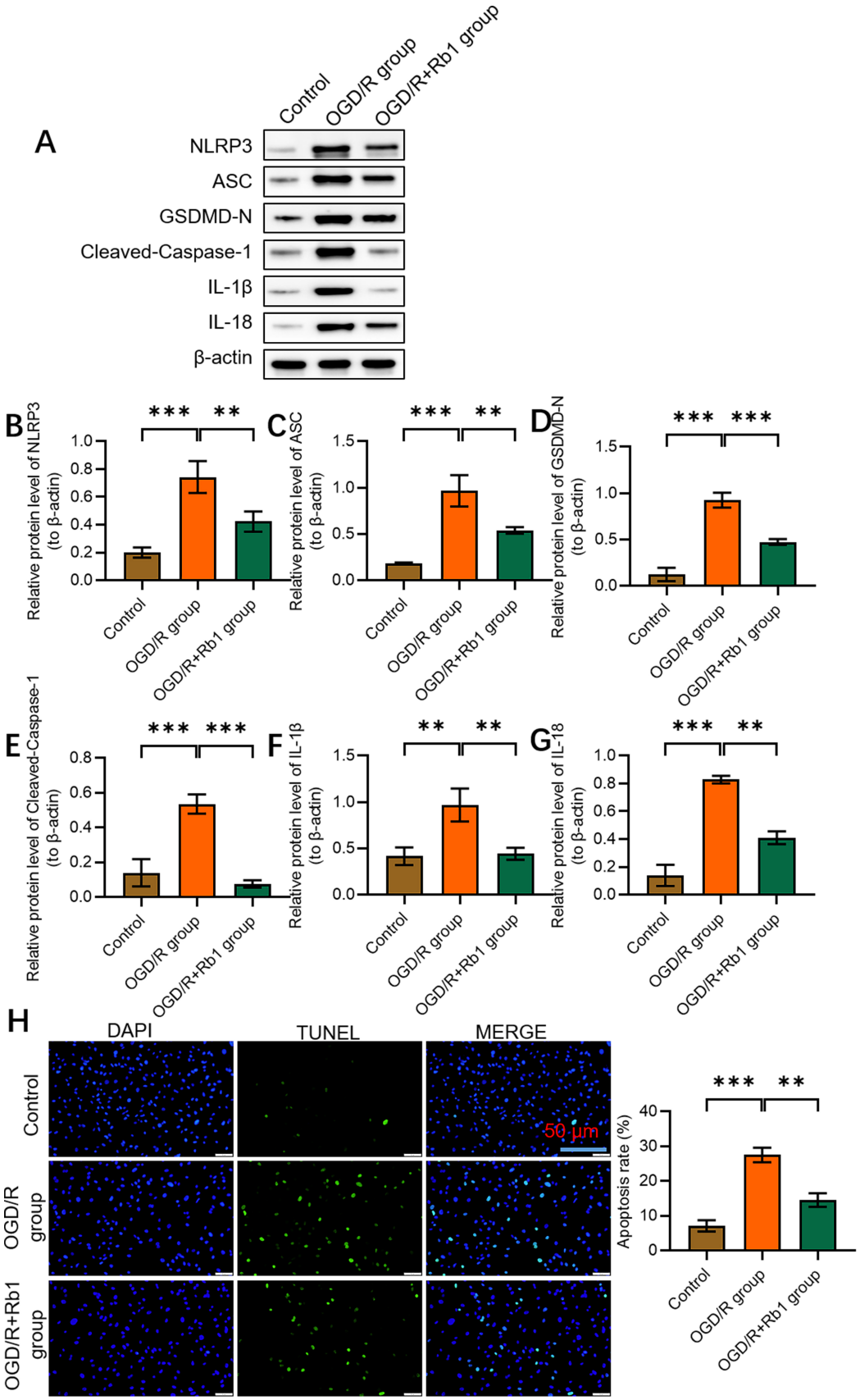

Fig. 3. Cell model results demonstrate the inhibition of pyroptosis in HT22 cells by ginsenoside Rb1. (A–G) Western blot images of NLRP3, ASC, GSDMD-N, Cleaved-Caspase-1, IL-1β, IL-18, and β-actin protein expression. (H) TUNEL staining confirmed the reduction of HT22 neuronal apoptosis by Rb1. N = 10, $^{**}p < 0.01$, $^{***}p < 0.001$. OGD/R, oxygen-glucose deprivation/reperfusion.

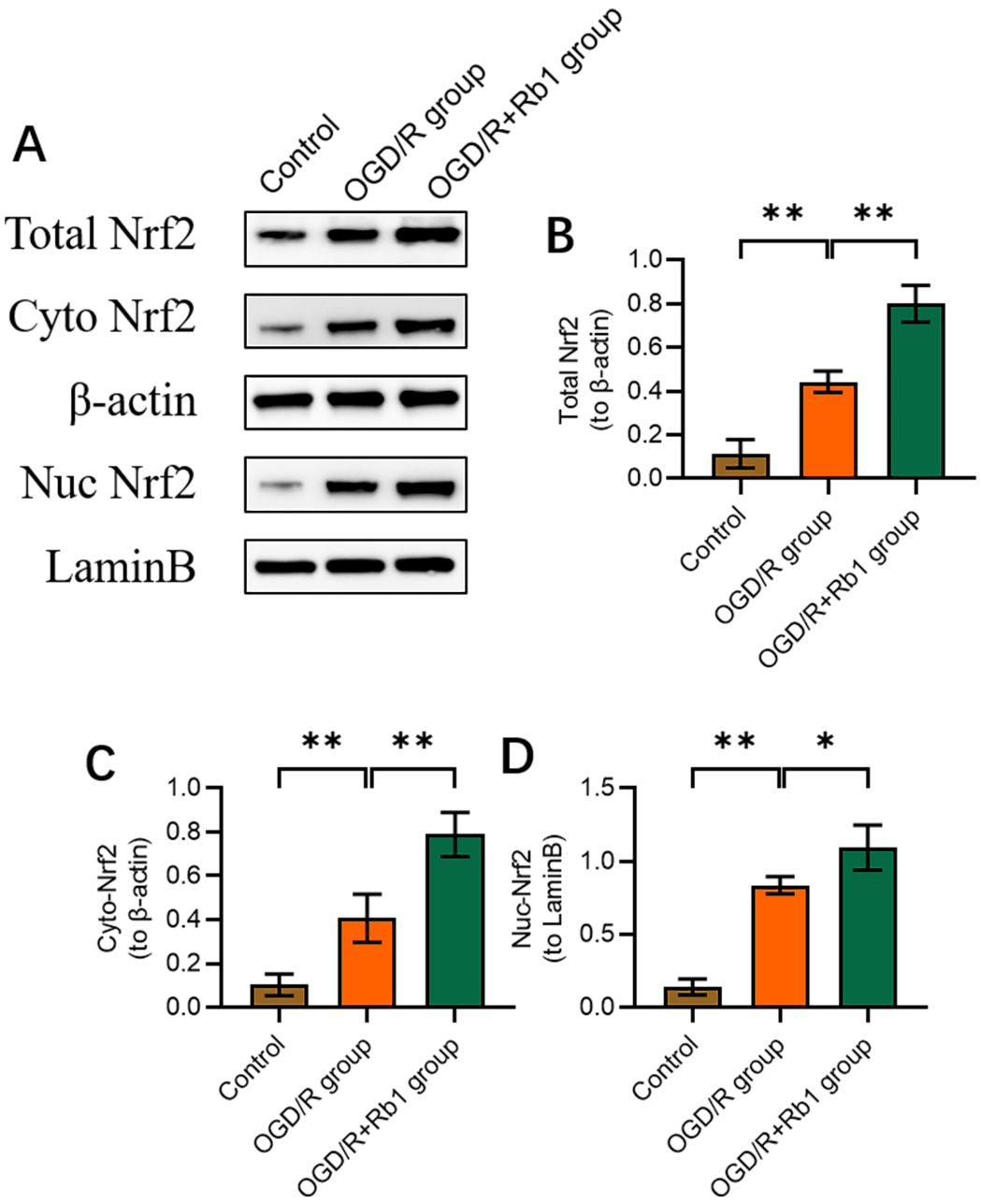

Fig. 4. Ginsenoside Rb1 increases nuclear respiratoty factor 2 (Nrf2) expression in OGD/R-injured neurons. (A) Upregulation of Nrf2 expression in the cytoplasm and nucleus by Rb1. (B) Total Nrf2 expression in cells. (C) Nrf2 expression in the cytoplasm. (D) Nrf2 expression in the nucleus. N = 10, *$p < 0.05$, **$p < 0.01$.

pyroptosis in HT22 cells after transfection of eEF1A2 followed by Rb1 treatment were examined using Western blot analysis. The experimental groups included the OGD group, OGD/R+Rb1 group, OGD/R+Rb1+OE-NC group, and OGD/R+Rb1+OE-eEF1A2 group. These proteins are crucial in cellular pyroptosis, and alterations in their expression levels can reflect the cellular pyroptotic state. Rb1 treatment demonstrated the ability to alleviate cellular pyroptosis and inflammatory responses. However, when eEF1A2 was overexpressed, as observed in the OGD/R+Rb1+OE-eEF1A2 group, there was a significant increase in NLRP3, ASC, GSDMD-N, and Cleaved-Caspase-1 expression ($p < 0.01$), indicating that eEF1A2 overexpression reversed the protective effect of Rb1, leading to the reactivation of pyroptosis and inflammatory responses (Fig. 7C–G). Thus, the experimental results suggest that eEF1A2 overexpression diminishes the protective effect of ginsenoside Rb1 on HT22 cells after OGD/R injury, further corroboratingthe hypothesis that ginsenoside Rb1 may alleviate CIRI by regulating the NRF2-A20-EEF1A2 axis and NLRP3.

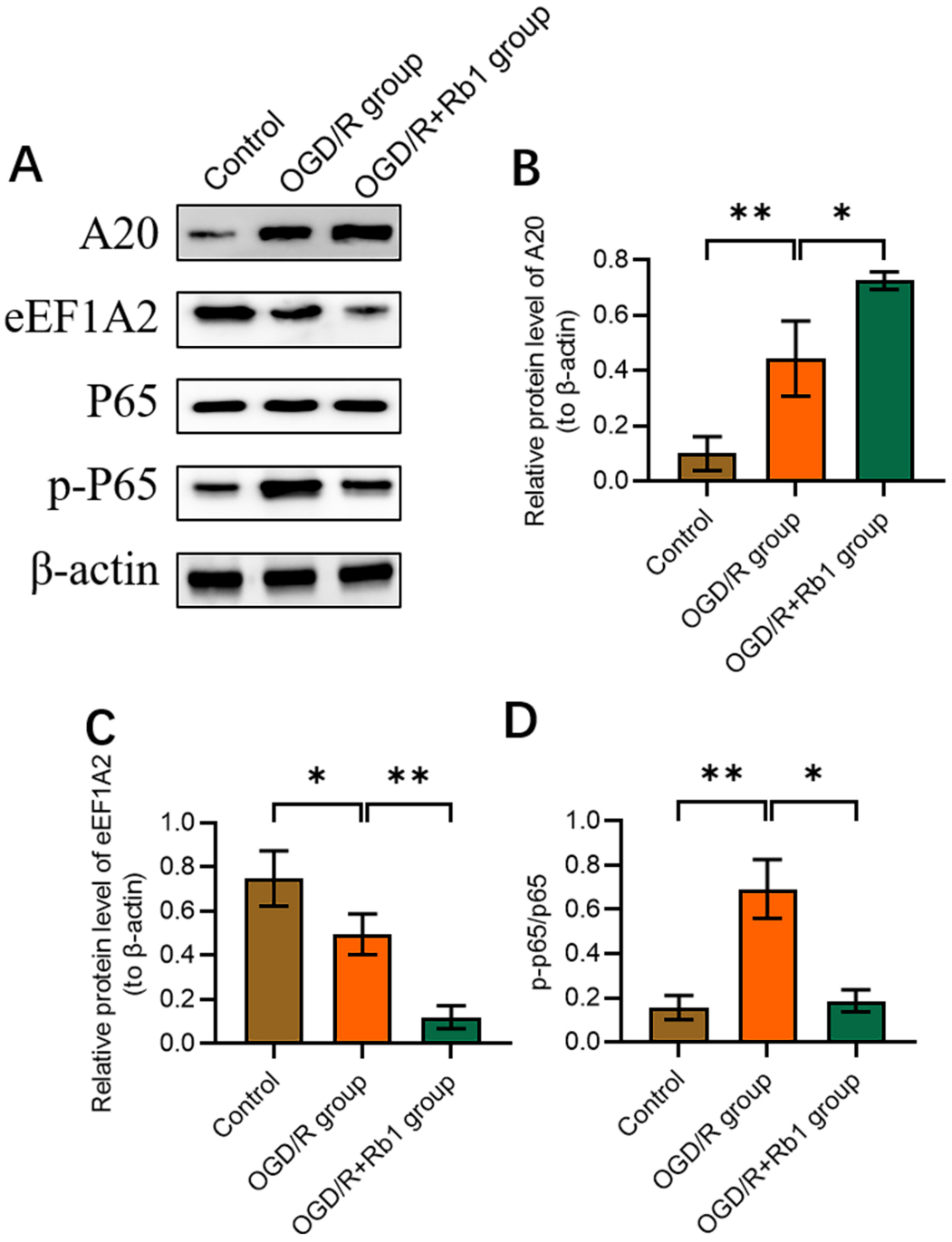

Fig. 5. Ginsenoside Rb1 upregulates TNFα-induced Protein 3 (TNFAIP3, aka A20) expression via nuclear respiratoty factor 2 (Nrf2), inhibiting eukaryotic translation elongation factor 1A2 (eEF1A2) and Phosphor (p)-p65 expression. (A) Upregulation of A20 expression and inhibition of eEF1A2 expression by Rb1. (B) A20 expression in cells. (C) eEF1A2 expression in cells. (D) p-p65/p65 expression. N = 10, *$p < 0.05$, **$p < 0.01$.

Discussion

CIRI is a prevalent and severe neurological disorder characterized by intricate pathophysiological mechanisms underlying its onset and progression [22]. Currently, the quest for efficacious treatment modalities to mitigate CIRI's detrimental effects on patients has emerged as a focal point of research interest [23]. Recent investigations have highlighted the potential neuroprotective properties of bioactive compounds found in natural remedies [24–26]. This study endeavors to elucidate the neuroprotective role of ginsenoside Rb1 in CIRI and scrutinize its mechanism of action. The principal findings of this study underscore that ginsenoside Rb1 attenuates cellular apoptosis and inflammatory responses induced by CIRI through modulation of the Nrf2/A20/eEF1A2 axis and NLRP3. Nrf2 binds to the pro-

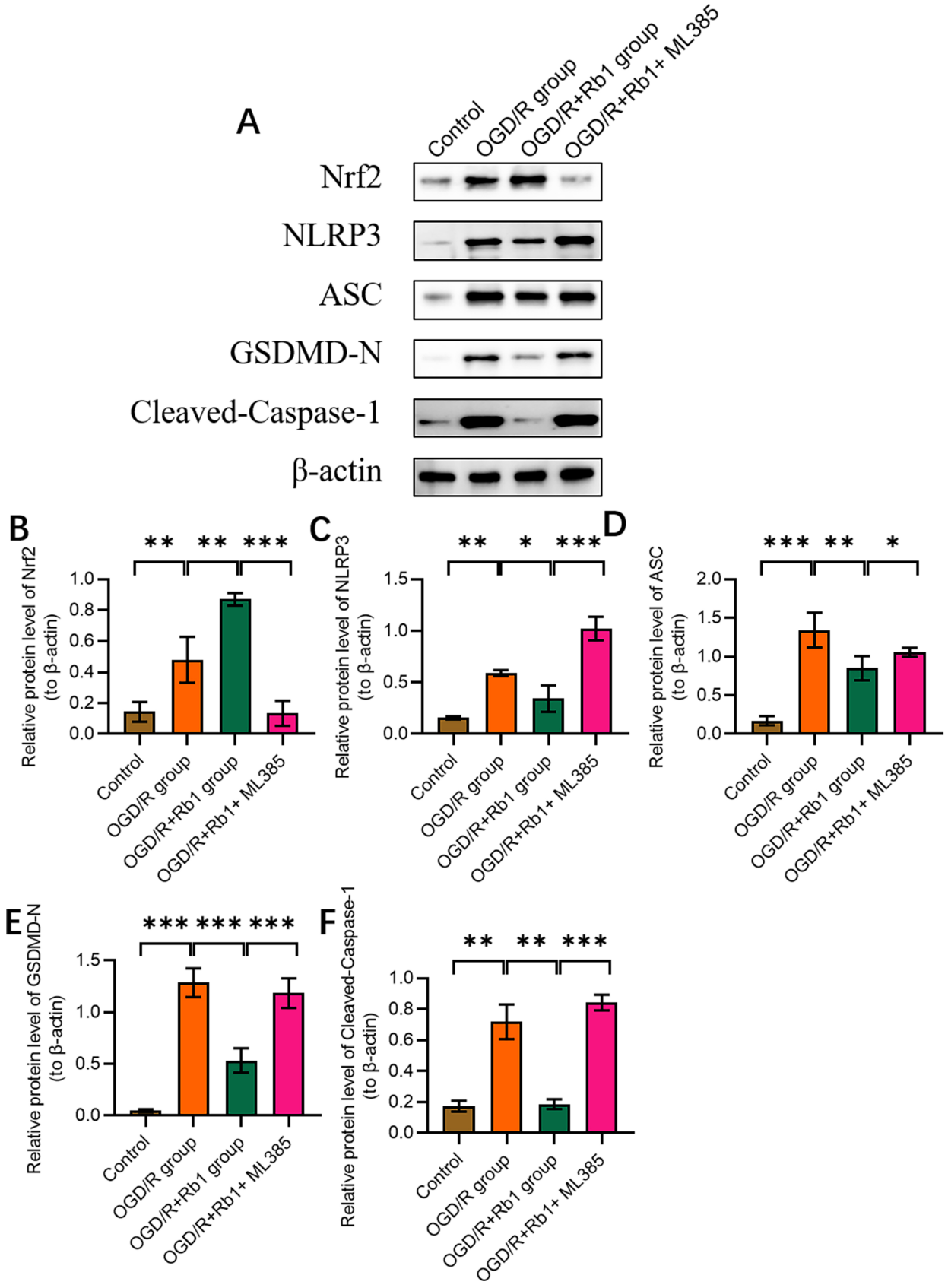

Fig. 6. Nrf2 inhibitor ML385 reverses the protective effect of ginsenoside Rb1 on OGD/R-induced HT22 cell damage. (A) Western blot analysis of changes in pyroptosis in HT22 cells treated with Nrf2 inhibitor ML385 followed by Rb1 treatment. (B–F) Expression analysis of Nrf2 (B), NLRP3 (C), ASC (D), GSDMD-N (E), and Cleaved-Caspase-1 (F). N = 3, *$p < 0.05$, **$p < 0.01$, ***$p < 0.001$.

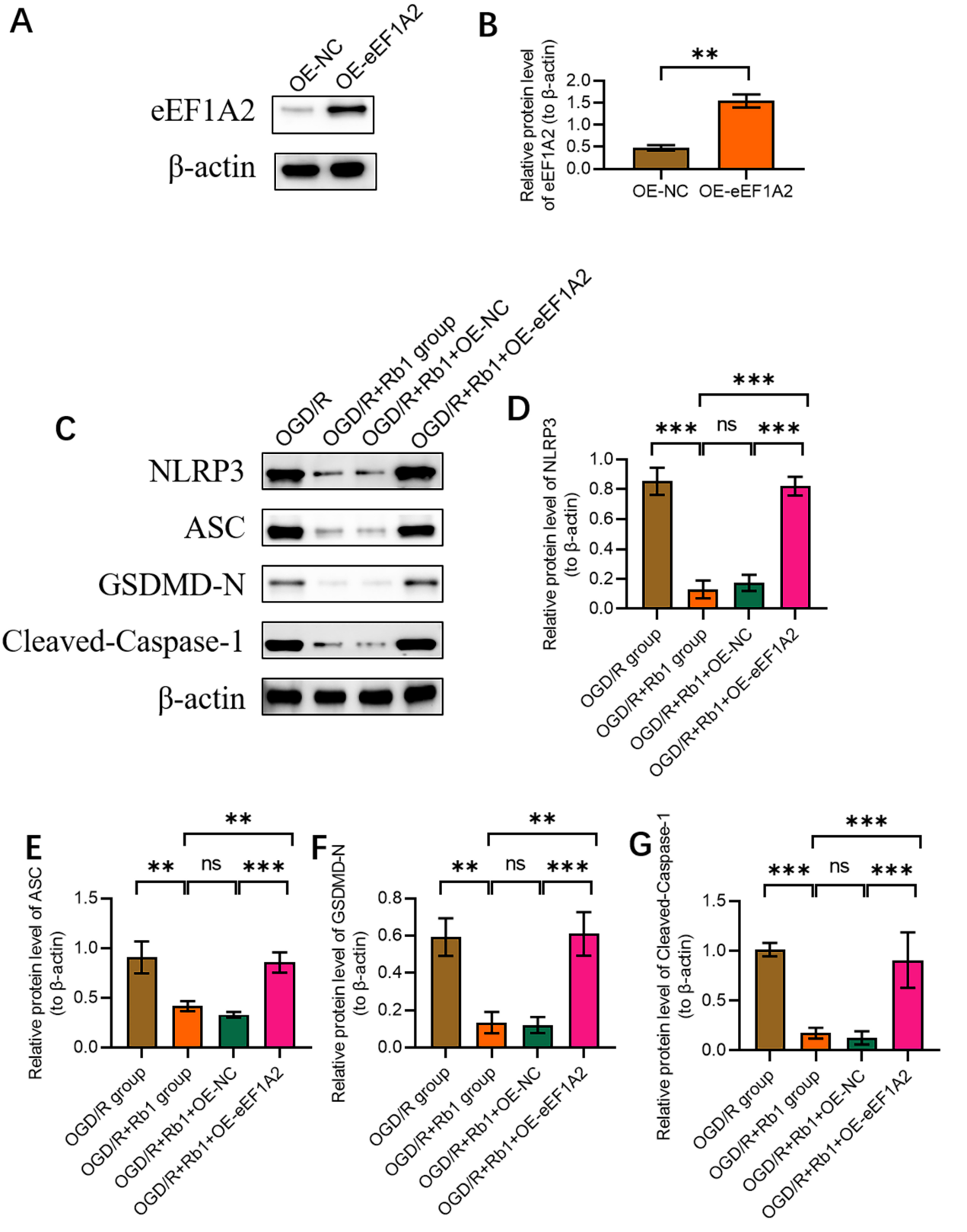

Fig. 7. Overexpression of eEF1A2 reduces the protective effect of ginsenoside Rb1 on OGD/R-induced HT22 cell damage. (A,B) Transfection efficiency of eEF1A2 overexpression plasmid in HT22 cells. (C) Western blot analysis of changes in pyroptosis in HT22 cells transfected with eEF1A2 followed by Rb1 treatment. (D–G) Expression analysis of NLRP3 (D), ASC (E), GSDMD-N (F), and Cleaved-Caspase-1 (G). N = 3, ns, no significant, $^{**}p < 0.01$, $^{***}p < 0.001$.

moter region of A20, thereby exerting transcriptional control over A20 expression. Furthermore, A20 interacts with eEF1A2 via its ZnF4 domain, facilitating the ubiquitination and subsequent degradation of eEF1A2 [27]. Additionally, research suggests that by modulating the NF-κB signaling pathway, NLRP3 inflammasome assembly is impeded, while eEF1A2 acts to inhibit NF-κB signaling [28]. In concert with our experimental findings, ginsenoside Rb1 activates the Nrf2 transcription factor, thereby bolstering antioxidative stress responses, and suppressing inflammatory reactions via A20 interaction. Moreover, ginsenoside Rb1 regulates eEF1A2 activity, thereby reducing the incidence of cellular apoptosis. Furthermore, ginsenoside Rb1 inhibits NLRP3 activation, consequently curtailing the release of inflammatory mediators.

The key findings of this study are aligned with prior literature. Firstly, ginsenoside Rb1, a natural compound, has garnered significant attention for its protective role against CIRI. Previous investigations have established that ginsenoside Rb1 mitigates CIRI by suppressing oxidative stress and inflammatory cascades. This study delves deeper into the molecular mechanisms underlying the regulatory effects of ginsenoside Rb1 on the Nrf2/A20/eEF1A2 axis and NLRP3, furnishing additional insights and evidence to support previous findings. Specifically, one study has elucidated that Rb1 inhibits the TLR4/MyD88/NF-KB and TLR4/TRIF/IRF-3 pathways in microglial cells, thereby ameliorating cerebral ischemia-reperfusion injury [29]. Furthermore, the neuroprotective action of Rb1 has been associated with the activation of the TLR4/MyD88 and SIRT1 signaling pathways [30]. These investigations serve as a guide for further experimental exploration.

Additionally, our study reveals that ginsenoside Rb1 confers neuroprotection by impeding the activation of NLRP3 inflammasomes. NLRP3 inflammasomes are pivotal inflammatory complexes whose activation precipitates inflammatory responses and fosters cellular apoptosis. Our experimental findings demonstrate that ginsenoside Rb1 treatment attenuates the expression and activation of NLRP3, thereby curtailing the release of inflammatory mediators and reducing the incidence of cellular apoptosis. This underscores the anti-inflammatory and anti-apoptotic properties of ginsenoside Rb1, mediated through the inhibition of NLRP3 inflammasome activation, thereby mitigating neuronal cell demise induced by CIRI. Nevertheless, further elucidation is warranted to explore the specific molecular mechanisms through which Rb1 activates Nrf2 or inhibits NLRP3, as well as its potential effects on alternative cell death pathways in HT22 cells.

The academic contributions of this study are predominantly manifested in the following aspects. Firstly, the investigation unveiled the multifaceted regulatory effects of ginsenoside Rb1 in CIRI, encompassing the activation of the Nrf2/A20/eEF1A2 axis and the suppression of NLRP3 activation. These findings offer novel insights and avenues for the management of CIRI. Secondly, the study conducted a comprehensive exploration into the pharmacological mechanisms of ginsenoside Rb1, elucidating its role in antioxidative stress and the attenuation of inflammatory responses. These revelations furnish significant cues for further inquiries into the pathogenesis and identification of therapeutic targets for related diseases.

There remain several limitations within this study. Primarily, the focus primarily centered on animal models, with no clinical trials conducted as of yet. Thus, further investigations are imperative to ascertain the precise efficacy and safety profile of ginsenoside Rb1 in human subjects. Secondly, the study did not delve into potential alternative regulatory mechanisms and signaling pathways, such as apoptosis-related factors and inflammatory mediators. Future inquiries could delve deeper into these mechanisms and explore the multi-target regulatory effects of ginsenoside Rb1. Moreover, this study did not ascertain alterations in the extracellular microenvironment and their impact on intercellular communication, an avenue slated for exploration in subsequent experiments. Additionally, combining ginsenoside Rb1 with other pharmaceuticals or treatment modalities might potentiate the therapeutic outcomes for CIRI. Furthermore, additional clinical investigations are warranted to validate the long-term efficacy and potential adverse effects of ginsenoside Rb1, thereby optimizing treatment strategies.

Conclusion

In summary, our study underscores the neuroprotective potential of ginsenoside Rb1 through its modulation of the Nrf2/A20/eEF1A2 axis and inhibition of NLRP3 inflammasome activation, thereby ameliorating brain damage induced by CIRI. These findings not only offer novel insights into CIRI treatment but also furnish scientific support for the potential therapeutic utility of ginsenoside Rb1. Nonetheless, despite the promising nature of our research outcomes, further investigations are imperative to validate these findings and assess the feasibility and safety of ginsenoside Rb1 in clinical applications.

Availability of Data and Materials

All experimental data included in this study can be obtained by contacting the authors if needed.

Author Contributions

HJH and YQY: data curation, formal analysis, investigation, writing – original draft, writing – review & editing. XZ and BZ: formal analysis, methodology, software. YY: conceptualization, methodology. BZ: conceptualization, visualization, writing – review & editing. YY: formal analysis, methodology, software. BZ: project administration, visualization. All authors contributed significantly

to editorial changes of important content. All authors read and approved the final manuscript. All authors have participated sufficiently in the work and agreed to be accountable for all aspects of the work.

Ethics Approval and Consent to Participate

This study has been approved by the ethics committee of Taizhou Enze Medical Center (Group), Approval No. Tzy-2020020.

Acknowledgment

Not applicable.

Funding

This research was funded by Taizhou Science and Technology Plan Class A (Brain protection mediated by ginsenoside Rb1 mediated by NLRP3 inflammasome mediated cell pyroptosis), Grant No. 21ywa53.

Conflict of Interest

The authors declare no conflict of interest.

References

[1] Jurcau A, Simion A. Neuroinflammation in Cerebral Ischemia and Ischemia/Reperfusion Injuries: From Pathophysiology to Therapeutic Strategies. International Journal of Molecular Sciences. 2021; 23: 14.

[2] Wu M, Gu X, Ma Z. Mitochondrial Quality Control in Cerebral Ischemia-Reperfusion Injury. Molecular Neurobiology. 2021; 58: 5253–5271.

[3] Liao S, Apaijai N, Chattipakorn N, Chattipakorn SC. The possible roles of necroptosis during cerebral ischemia and ischemia / reperfusion injury. Archives of Biochemistry and Biophysics. 2020; 695: 108629.

[4] Hou Y, Wang Y, He Q, Li L, Xie H, Zhao Y, *et al*. Nrf2 inhibits NLRP3 inflammasome activation through regulating Trx1/TXNIP complex in cerebral ischemia reperfusion injury. Behavioural Brain Research. 2018; 336: 32–39.

[5] Xu Y, Gao X, Wang L, Yang M, Xie R. Bakuchiol ameliorates cerebral ischemia-reperfusion injury by modulating NLRP3 inflammasome and Nrf2 signaling. Respiratory Physiology & Neurobiology. 2021; 292: 103707.

[6] Shi M, Wang J, Bi F, Bai Z. Diosmetin alleviates cerebral ischemia-reperfusion injury through Keap1-mediated Nrf2/ARE signaling pathway activation and NLRP3 inflammasome inhibition. Environmental Toxicology. 2022; 37: 1529–1542.

[7] Xiao L, Dai Z, Tang W, Liu C, Tang B. Astragaloside IV Alleviates Cerebral Ischemia-Reperfusion Injury through NLRP3 Inflammasome-Mediated Pyroptosis Inhibition via Activating Nrf2. Oxidative Medicine and Cellular Longevity. 2021; 2021: 9925561.

[8] She Y, Shao L, Zhang Y, Hao Y, Cai Y, Cheng Z, *et al*. Neuroprotective effect of glycosides in Buyang Huanwu Decoction on pyroptosis following cerebral ischemia-reperfusion injury in rats. Journal of Ethnopharmacology. 2019; 242: 112051.

[9] Sun R, Peng M, Xu P, Huang F, Xie Y, Li J, *et al*. Low-density lipoprotein receptor (LDLR) regulates NLRP3-mediated neuronal pyroptosis following cerebral ischemia/reperfusion injury. Journal of Neuroinflammation. 2020; 17: 330.

[10] Ahmed T, Raza SH, Maryam A, Setzer WN, Braidy N, Nabavi SF, *et al*. Ginsenoside Rb1 as a neuroprotective agent: A review. Brain Research Bulletin. 2016; 125: 30–43.

[11] Mohanan P, Subramaniyam S, Mathiyalagan R, Yang DC. Molecular signaling of ginsenosides Rb1, Rg1, and Rg3 and their mode of actions. Journal of Ginseng Research. 2018; 42: 123–132.

[12] Gong L, Yin J, Zhang Y, Huang R, Lou Y, Jiang H, *et al*. Neuroprotective Mechanisms of Ginsenoside Rb1 in Central Nervous System Diseases. Frontiers in Pharmacology. 2022; 13: 914352.

[13] Han Y, Li X, Yang L, Zhang D, Li L, Dong X, *et al*. Ginsenoside Rg1 attenuates cerebral ischemia-reperfusion injury due to inhibition of NOX2-mediated calcium homeostasis dysregulation in mice. Journal of Ginseng Research. 2022; 46: 515–525.

[14] Zhang R, Chen DY, Luo XW, Yang Y, Zhang XC, Yang RH, *et al*. Comprehensive Analysis of the Effect of 20(*R*)-Ginsenoside Rg3 on Stroke Recovery in Rats via the Integrative miRNA-mRNA Regulatory Network. Molecules (Basel, Switzerland). 2022; 27: 1573.

[15] Ardiningtyas SA, Arista NID. Kajian metabolit sekunder tanaman ginseng Korea dan Indonesia sebagai peningkat imun tubuh. Holistic: Journal of Tropical Agriculture Sciences. 2023; 1.

[16] Xie W, Wang X, Xiao T, Cao Y, Wu Y, Yang D, *et al*. Protective Effects and Network Analysis of Ginsenoside Rb1 Against Cerebral Ischemia Injury: A Pharmacological Review. Frontiers in Pharmacology. 2021; 12: 604811.

[17] Yang C, Mo J, Liu Q, Li W, Chen Y, Feng J, *et al*. TXNIP/NLRP3 aggravates global cerebral ischemia-reperfusion injury-induced cognitive decline in mice. Heliyon. 2024; 10: e27423.

[18] Li Y, Xiang LL, Miao JX, Miao MS, Wang C. Protective effects of andrographolide against cerebral ischemia reperfusion injury in mice. International Journal of Molecular Medicine. 2021; 48: 186.

[19] Li YH, Li YY, Fan GW, Yu JH, Duan ZZ, Wang LY, *et al*. Cardioprotection of ginsenoside Rb1 against ischemia/reperfusion injury is associated with mitochondrial permeability transition pore opening inhibition. Chinese Journal of Integrative Medicine. 2016. (online ahead of print)

[20] Jiang Y, Zhou Z, Meng QT, Sun Q, Su W, Lei S, *et al*. Ginsenoside Rb1 Treatment Attenuates Pulmonary Inflammatory Cytokine Release and Tissue Injury following Intestinal Ischemia Reperfusion Injury in Mice. Oxidative Medicine and Cellular Longevity. 2015; 2015: 843721.

[21] Wang XF, Liu XJ, Zhou QM, Du J, Zhang TL, Lu YY, *et al*. Ginsenoside rb1 reduces isoproterenol-induced cardiomyocytes apoptosis in vitro and in vivo. Evidence-based Complementary and Alternative Medicine: ECAM. 2013; 2013: 454389.

[22] Zhao H, Deng L, Chen S, Wang X, Dong Z. Neuroprotection of β-caryophyllene against cerebral ischemia/reperfusion injury by inhibiting P38 MAPK/NLRP3 signaling pathway. Neuroreport. 2023; 34: 617–623.

[23] Lu H, Wang B. SIRT1 exerts neuroprotective effects by attenuating cerebral ischemia/reperfusion-induced injury via targeting p53/microRNA-22. International Journal of Molecular Medicine. 2017; 39: 208–216.

[24] Susita O, Khiong TK. Biologi Molekuler Stroke Iskemik Ditinjau Dari Teori Medis Barat Dan Tcm. Journal of Comprehensive Science (JCS). 2023; 2: 1104–1112.

[25] Xu H, Sun H, Chen SH, Zhang YM, Piao YL, Gao Y. Effects of acupuncture at Baihui (DU20) and Zusanli (ST36) on the expression of heat shock protein 70 and tumor necrosis factor α in the peripheral serum of cerebral ischemia-reperfusion-injured rats. Chinese Journal of Integrative Medicine. 2014; 20: 369–374.

[26] Li XH, Yin FT, Zhou XH, Zhang AH, Sun H, Yan GL, *et al*. The Signaling Pathways and Targets of Natural Compounds from Traditional Chinese Medicine in Treating Ischemic Stroke. Molecules (Basel, Switzerland). 2022; 27: 3099.

[27] Bai W, Huo S, Zhou G, Li J, Yang Y, Shao J. Biliverdin modulates the Nrf2/A20/eEF1A2 axis to alleviate cerebral ischemia-reperfusion injury by inhibiting pyroptosis. Biomedicine & Pharmacotherapy. 2023; 165: 115057.

[28] Tan Y, Sun R, Liu L, Yang D, Xiang Q, Li L, *et al*. Tumor suppressor DRD2 facilitates M1 macrophages and restricts NF-κB signaling to trigger pyroptosis in breast cancer. Theranostics. 2021; 11: 5214–5231.

[29] Guan Y, Cao YL, Liu JW, Liu LT, Zheng YJ, Ma XF, *et al*. Ginsenoside Rg1 attenuates cerebral ischemia-reperfusion injury through inhibiting the inflammatory activation of microglia. Experimental Cell Research. 2023; 426: 113552.

[30] Cheng Z, Zhang M, Ling C, Zhu Y, Ren H, Hong C, *et al*. Neuroprotective Effects of Ginsenosides against Cerebral Ischemia. Molecules (Basel, Switzerland). 2019; 24: 1102.